https://ijrps.com

ISSN: 0975-7538
Research Article

Assessment of genotoxicity of engineered nanoparticles (cadmium sulphide – CdS and copper oxide - CuO) using plant model (*Coriandrum sativum* L.)

Ankita Pramanik[1], Animesh Kumar Datta[1]*, Sudha Gupta[2], Bapi Ghosh[1], Debadrito Das[1], Divya Vishambhar Kumbhakar[1]

[1]Department of Botany, Cytogenetics, Genetics and Plant Breeding Section, University of Kalyani, Kalyani - 741235, West Bengal, India

[2]Department of Botany, Pteridology and Palaeobotany Section, University of Kalyani, Kalyani - 741235, West Bengal, India

ABSTRACT

Engineered semiconductor nanoparticles (CdS-NPs and CuO-NPs) are synthesized following wet chemical microwave assisted techniques and opto-physically characterized (using UV-vis, FTIR, XRD, DLS and FESEM) for assurance of standard nano quality. The accumulation of the prepared NPs in seedling ash in the form of metallic cataions is studied using atomic absorption spectroscopy. Furthermore, genotoxicity (assessing micronuclei frequency in somatic cells and using comet assay) including cellular stress (accumulation of hydrogen peroxide and malondialdehyde as well as Evans blue uptake) and the extent of defense enzyme activation are also studied using plant species (*Coriandrum sativum* L.; Apiaceae; spice and leafy vegetable yielding plant species of commerce) as host system. Results suggest prevalence of cellular stress environment as well as genotoxicity irrespective of host defense enzyme activity. Toxicity of NPs can well be used for pharmacological application and drug designing.

Keywords: Comet assay; *Coriandrum sativum*, Micronuclei; Nanoparticles, Oxidative stress.

INTRODUCTION

Release of nanoparticles (NPs) in eco-environmental inter-collegium through various natural processes and anthropogenic activities (Nowack and Bucheli., 2007; Tervonen et al., 2009, Lidén., 2011) impose a serious threat on biotic community following generation of highly reactive molecules including superoxides and various reactive oxygen species in the form of oxidative stress (Fahmy and Cormier., 2009). Cellular stress due to NPs induced dysregulation of ionic equilibrium in the host cytoplasm results in deviation of normalized cellular processes, DNA damage and cellular toxicity (Manke et al., 2013; Ali et al., 2015) affecting overall health of the biological system. Stress induction and genotoxicity due to NPs are studied mostly in animal models and cell lines (Ghosh et al., 2010; Dobrzyńska et al., 2014; Valencia-Quintana et al., 2016) but rarely in plant species (Ventura et al., 2013; Das et al., 2017). Rooted plants as the immediate site of interaction with soil deposited NPs, can be used as efficient models (due to their cost effectivity and applicational simplicity) for determination of nanomaterial mediated stress and toxicity. Nanotoxicity can be effectively explored against human pathogenic bacteria as an application in pharmacological sciences and drug designing (Kumbhakar et al., 2017). With the view to it, present investigation is designed to assess the stress generation potentiality of cadmium sulphide (CdS) and copper oxide (CuO) NPs (wet chemical synthesized and opto-physical characterized) and subsequent antioxidant responsiveness by the host (*Coriandrum sativum* L. Family: Apiaceae; spice and leafy vegetable yielding plant species of commerce with immense therapeutic uses– Pathak et al., 2011; Rajeshwari and Andallu., 2011) and genotoxicity (assessing micronuclei frequency in somatic cells and using alkaline comet assay).

* Corresponding Author
Email: dattaanimesh@gmail.com
Contact: +91 9831483747
Received on: 25.10.2017
Revised on: 06.12.2017
Accepted on: 09.12.2017

MATERIALS AND METHODS

Germplasm source

Seeds (moisture content: 13.60%; seed size: length–5.04 ± 0.13 mm, breadth– 3.47 ± 0.08 mm; seed color assessed from RAL color chart: Sand yellow-RAL-1002-198-166-100) of *Coriandrum sativum* L. (Family: Apiaceae) were obtained (as breeder's seeds) from Pulses and Oil Seeds Research Station, Department of Agriculture, Govt. of West Bengal, Berhampore, Murshidabad.

Preparation of nanoparticles (NPs)

CdS-NPs were prepared following the methodology adopted by Halder et al. (2015). For the purpose, NPs were wet chemically co-precipitated by regulating the

reaction kinetics of cadmium acetate [$(CH_3COO)_2Cd$, AR grade–source of Cd^{+2}] and sodium sulphide ($Na_2S;9H_2O$, AR grade–source of S^{2-}) within the SDS (Sodium dodecyl sulphate) capping closed system.

For synthesis of CuO-NPs, a wet chemical-microwave assisted technique was optimized. For the purpose, ammonium hydroxide (10.0%– AR grade) solution was added (drop wise) into copper chloride solution (0.01 M, AR–grade) following continuous stirring for 4 h. Resultant suspension was microwaved for 10 mins under medium power mode at 230 Volt–800 Watt. Development of blackish coloration of the suspension is the indicator of the growth of CuO-NPs.

Bulk CdS and CuO were prepared by the respective methods without the application of capping agents (sodium dodecyl sulphate-SDS).

Characterization of the prepared NPs

Both the synthesized NPs were opto-physically characterized using UV–visible (UV-vis, Shimadzu UVPC-1601) and fourier transform infra-red (FTIR, Jasco FT/IR-6300) spectrometers, X-ray diffractometers (XRD, Shimadzu LabX, λ=1.5406 Å, 2θ from 10^o–80^o), dynamic light scattering analyzer (DLS, Delsa™ Nano C, Beckman Coulter) and field emission scanning electron microscope (FESEM, JEOL JSM-7600F) for assurance of nano quality.

For FTIR analysis, powdered NPs were diluted in KBr (IR–grade). From X-ray scattering plot, size of nano crystal (D_{nkl}) was estimated using Debye– Scherrer equation ($D_{nkl} = k\lambda/\beta\cos\theta$, where λ = wavelength of Cu K_α radiation, β = full width of half maximum intensity, θ = diffraction angle of considered diffraction peak and k = shape factor constant). For nano crystal morphology, FESEM scanning was performed on a dropped dried NPs mounted carbon coated copper grid (TED PELLA INC.USA).

Bulk CdS and CuO were oven dried (80º ± 1ºC) and the size measurements were performed using stereo microscope (Stereo Zoom® Leica S8 APO).

Treatments

Dry seeds of *C. sativum* were exposed to CdS- and CuO-NPs (0.25, 0.50 and 1.00 µg/ml, 2 and 4 h durations). Dry control and bulk CdS and CuO controls (0.25 µg/ml, 2 h) were kept for assessment. Doses were selected after pilot trials.

Assessment of CdS- and CuO-NPs uptake in seedlings

A weight of 0.02 g ash (15 days old seedling, dried at 400ºC for 24 h) from each treatment including bulk controls was digested in 25 ml tri-acid mixture (70.4% nitric acid:96.0% sulphuric acid:61.3% perchloric acid::3:3:1) following volume reduction to 5 ml under a fume hood (80ºC). Acid digested solutions were cooled to room temperature (27º ± 1ºC) and were diluted upto 25 ml using deionized water. Diluted samples were filtered using Whatman filter paper (No. 42) and crystal clear solutions were used for Atomic absorption spectroscopic analysis (Spectra AAS 240, Agilent technologies; detection wavelength 326.1 nm and 324.7 nm for Cd^{2+} and Cu^{2+} respectively).

Assessment of stress induction by NPs

Root cell viability estimation

Root cell viability was assessed following Evans blue test (Tamás et al., 2004). For the purpose, roots from each treatment including controls were cut and dipped in 0.2% (w/v) dye solution for overnight at room temperature (27˚ ± 1˚C). Stained roots were washed in ddH_2O for removal of loosely attached stain from root surfaces. Root tips were subsequently cut and incubated in N, N dimethyl formamide solution (1000 µl) for overnight at 4˚C. After incubation, released dye (Evans blue) was estimated spectroscopically at 600 nm and the data obtained were represented as percent of control (untreated control).

Measurement of endogenous hydrogen peroxide (H_2O_2)

H_2O_2 accumulation in treated seedlings was measured according to Brennan and Frenkel (1977). For the purpose, 10 days old seedlings (0.2 g) from each treatment (including control) were homogenized in 5 ml chilled acetone and filtered using Whatman Filter Paper (No.42). Reaction mixture was prepared by 250 µl filtrate mixed with 250 µl titanium reagent (20% titanium tetrachloride in concentrated HCl–v/v) and 500 µl ammonia water (concentrated). Resultant reaction mixture was then centrifuged at 7000 rpm (30 min). Precipitates were dissolved in 2 N sulphuric acid. H_2O_2 content was recorded from the optical density measured for each final suspension at 415 nm.

Measurement of Malondialdehyde (MDA)

Endogenous MDA content in NPs treated seedlings was quantified as per Heath and Packer (1968). For the study, about 0.2 g seedlings (10 days old) from each treatment (including control) were homogenized in 80% ice-cold ethanol and centrifuged at 6000 rpm for 15 mins. Supernatants were collected with trichloro-acetic acid (20%) solution containing thiobarbituric acid (5% w/v). Resultant mixtures were heated in water bath at 90˚C for 1h and immediately transferred to ice-bath. Ice cooled samples were re-centrifuged at 6000 rpm for 5 mins and optical density was recorded at 532 and 600 nm.

Anti-oxidant enzyme responses

Extraction and estimation of ascorbate peroxidase (APX)

Extraction

APX enzyme [EC 1.11.1.11] extraction was accomplished by homogenizing 0.4 g frozen seedlings (10 days old) in potassium phosphate buffer (50 mM, pH 7.8) consisting

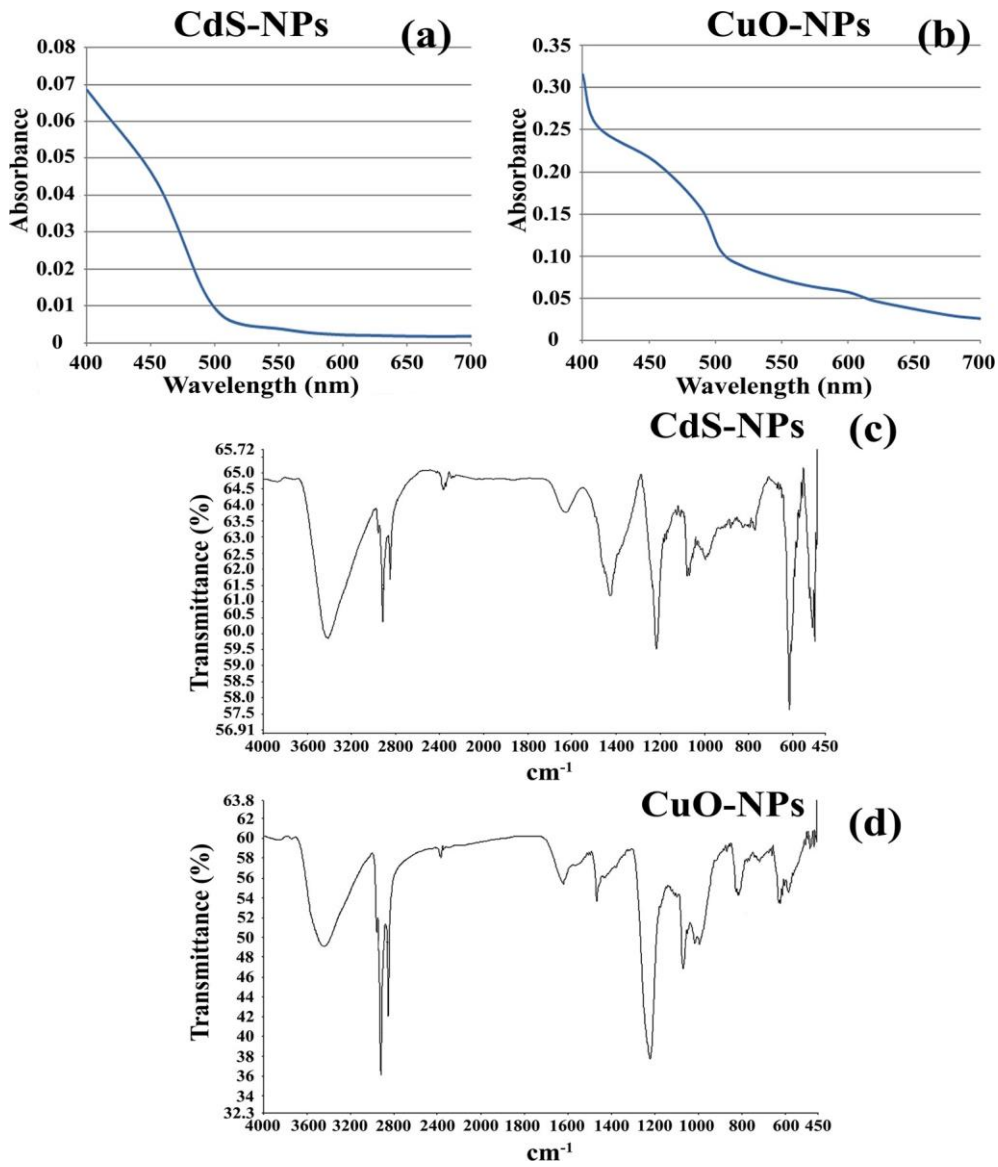

Figure 1: UV-Vis absorption plots (a-b) and FTIR plots (c-d)

4 mM ascorbate, 2 mM ethyldiaminetetracetic acid (EDTA), 2 mM dithiothreitol (DTT) and 2% w/v polyvinylpyrrollidone (PVP). Total soluble protein content in seedlings was estimated following Lowry et al. (1951) using BSA (Bovine Serum Albumin) as standard curve.

Estimation

APX reaction kinetics was measured as per Nakano and Asada (1981). For the purpose, 800 µl potassium phosphate buffer (50 mM, pH 7.0), 200 µl EDTA (1 mM), 760 µl ascorbate (1 mM) and 40 µl H_2O_2 were used for preparation of 1.8 ml pre-reaction mixture. Oxidation reaction was initiated by introducing 100 µl enzyme extract into the pre-reaction solution. APX kinetics was estimated by measuring decrease in absorption efficiency at 290 nm (ε=2.8 $mM^{-1}cm^{-1}$). Reactivity was represented as µmol ascorbate oxidized under unit time and per mg of protein (min/mg protein).

Extraction and estimation of Monodehydroascorbate reductase (MDAR), glutathione reductase (GR) and total superoxide dismutase (tSOD)

Extraction

For enzyme extraction, 10 days old frosted (-4ºC) seedlings (0.4 g) were homogenized in 1.5 ml chilled potassium phosphate buffer (pH 7.8; consisting 2 mM EDTA, 2 mM DTT and 2.0% PVP). Resultant suspensions were centrifuged at 15000 rpm for 30 mins at 4˚C. Clear supernatants were used for estimation of enzyme activity.

Estimation of enzyme kinetics

MDAR

MDAR [EC 1.6.5.4] activity was measured as per Miyake and Asada (1992). MDHA was measured spectroscopically by reading the absorbance at 265 nm. For the study, reaction mixture was prepared using 340 µl HEPES-KOH buffer (50 mM, pH 7.6), 60 µl NADPH (0.1 mM), 560 µl ascorbate (2.5 mM) and 20 µl enzyme extract. MDAR activity was represented as µmol NADPH oxidized under unit time and mg of protein (min/mg protein).

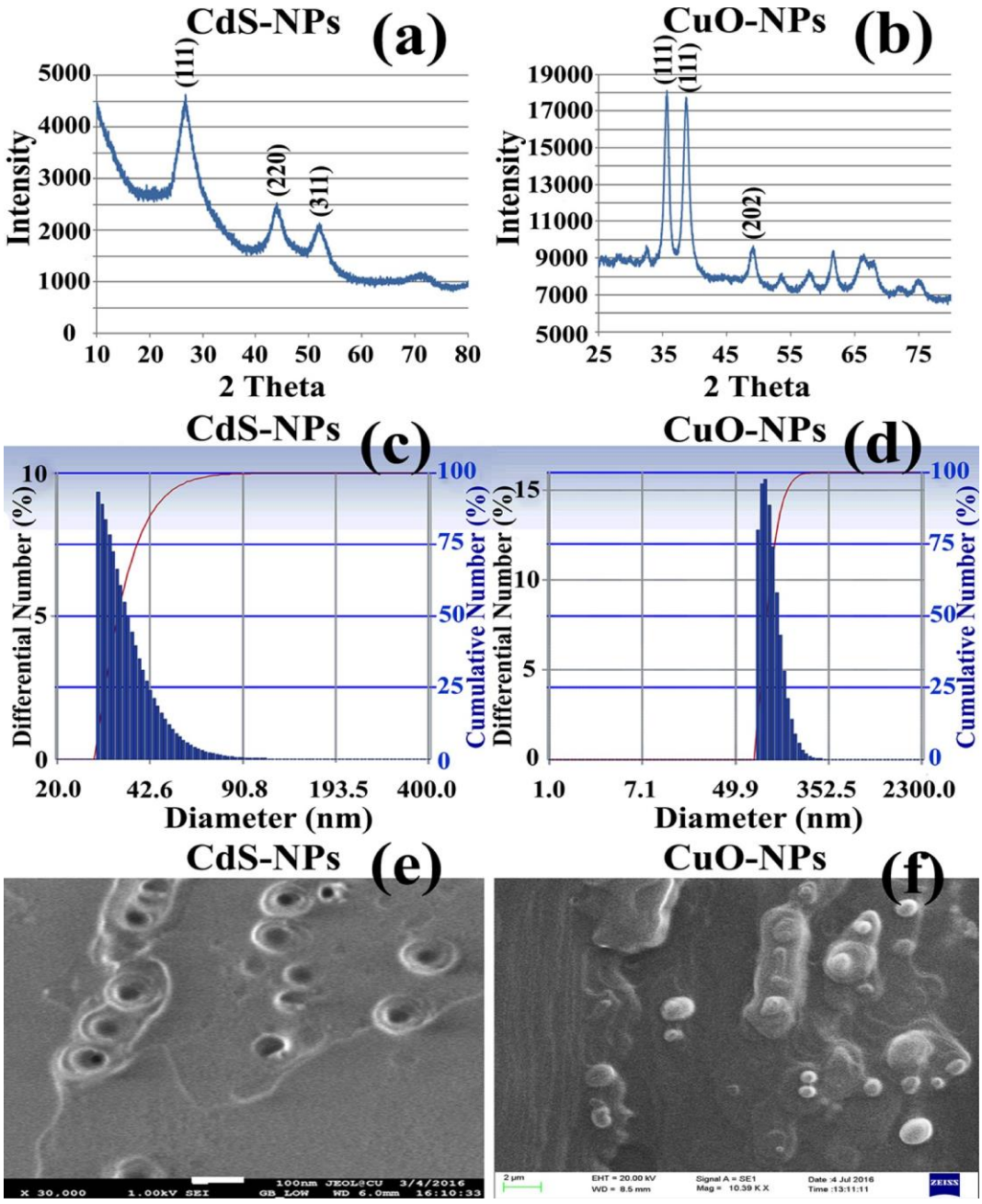

Figure 2: X-ray diffraction patterns showing crystal faces of NPs (a-b); DLS plots demonstrating particle size distribution (c-d); FESEM manifesting nanocrystal morphology (e-f)

GR

GR [EC 1.8.5.1] reactivity was measured following Carlberg and Mannervik (1985). For GR activity, pre-reaction mixture (comprising of 750 µl 0.2 M potassium phosphate buffer, 2 mM EDTA, 75 µl 2 mM NADPH and 75 µl 20 mM oxidised glutathione; pH 7.0) was prepared and enzyme extract (100 µl) was added to it. Reduction in absorbance was recorded at 340 nm for 2 mins. GR reaction kinetics was estimated using extinction coefficient of NADPH as 6.2 mM^{-1} cm^{-1}.

tSOD

Total SOD [EC 1.15.1.1] activity was monitored according to Beyer and Fridovich (1987). For the purpose, about 1000 µl of pre-reaction mixture was preparedby using 880 µl potassium phosphate buffer (50 mM), 50 µl L- methionine (10 mM), 30 µl nitroblue tetrazolium–NBT (60 µM), 30 µl Triton-X 100 (0.05 %) and 20 µl enzyme extract. Enzymatic reaction was initiated by adding 0.05% riboflavin and the resultant solutions were exposed to 20 W fluorescent lamp (10 mins). Sample absorbance was recorded at 560 nm. SOD activity was represented as unit (1 unit equals to I_{50}–50% inhibition of NBT reduction by SOD) per mg of protein (U/mg protein).

Extraction and estimation of glutathione S-transferase (GST)

Extraction

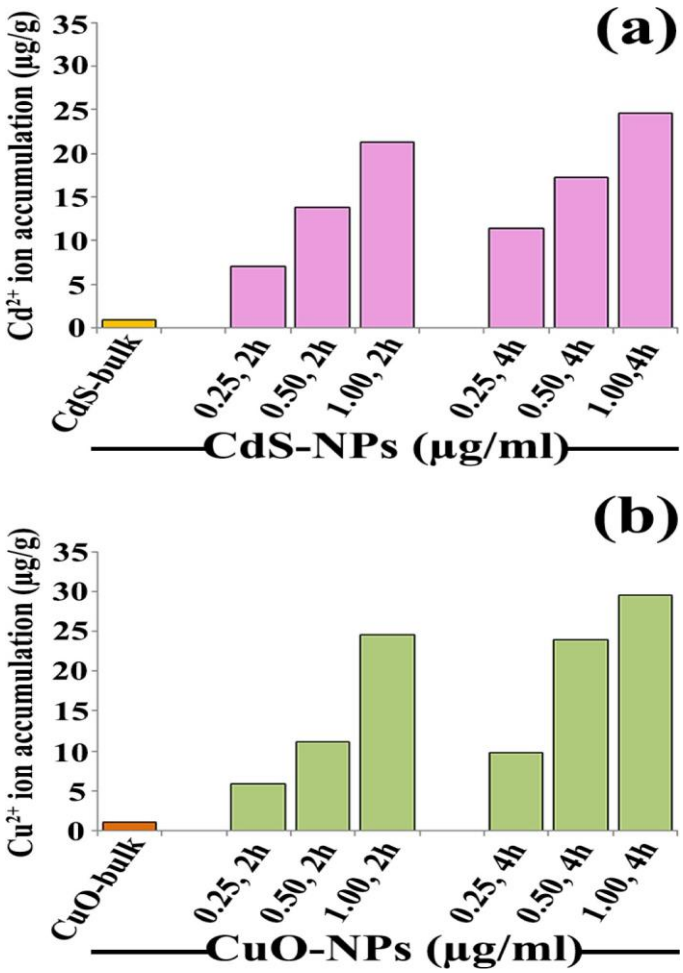

Figure 3: NPs accumulation in seedling ash in the form of metallic cataions (a-b)

Enzyme (EC 2.5.1.18) extraction is performed from 0.4 g frosted seedlings grounded in 1000 µl extraction buffer [potass ium phosphate buffer (0.1 M, pH 7.0) comprising EDTA and PVP]. Resultant solution was centrifuged at 15000 rpm at 4˚C for 15 mins. Clear supernatants were used for assessment of enzyme kinetics.

Estimation

GST enzyme was quantified as per Aebi (1983). For the purpose, pre-reaction solution was prepared by mixing 1.78 ml potassium phosphate buffer (50 mM, pH 7.5) and 20 µl 1-chloro-2,4-di nitrobenzene (cDNB, 1 mM). Reaction was triggered following addition of reduced glutathione (GSH, 1 mM) and 100 µl enzyme extract. Optical density was recorded at 340 nm for measurement of GST activity.

Assessment of genotoxicity

Study of micronuclei from root tip cells

Control and treated (5 roots in each case) root tips stained in 9:1 aceto-orcein – HCl mixture following hydrolysis were assessed to ascertain frequency of micronuclei in resting cells as suggested by Ghosh et al. (2017).

Measurement of tail DNA from comet assay

Genotoxic potentiality of CdS- and CuO-NPs was estimated using alkaline comet assay (Pourrut et al., 2015) from root tip nuclei. Per cent of tail DNA were measured by "Komet 4" software. Three replicas for each treatment (including dry and bulk controls) were kept under assessment (data pooled over the replicas).

Statistical analyses

Duncan's Multiple Range Test (IBM® SPSS Statistics Software) was used to assess significant variation (p<0.05) between mean values of controls and treatments for different parameters namely, root cell viability, oxidative stress, antioxidant enzymes and tail DNA. Length of tail DNA was converted to percentage in relation to respective undamaged nuclei head.

RESULTS AND DISCUSSION

Characterization

CdS- and CuO-NPs show definite visible absorption edges drawn from intensity maxima at 512 nm and 538 nm respectively (Fig. 1a-b). Sharp increase in spectrum absorbance towards lower wavelength region reveals blue-shifting phenomenon attributing to the reduced nanocrystal sizing effect for both the studied NPs (Duchaniya., 2014; Dagher et al., 2014). Infra-red transmission efficiency patterns exhibit multiple inverse peak

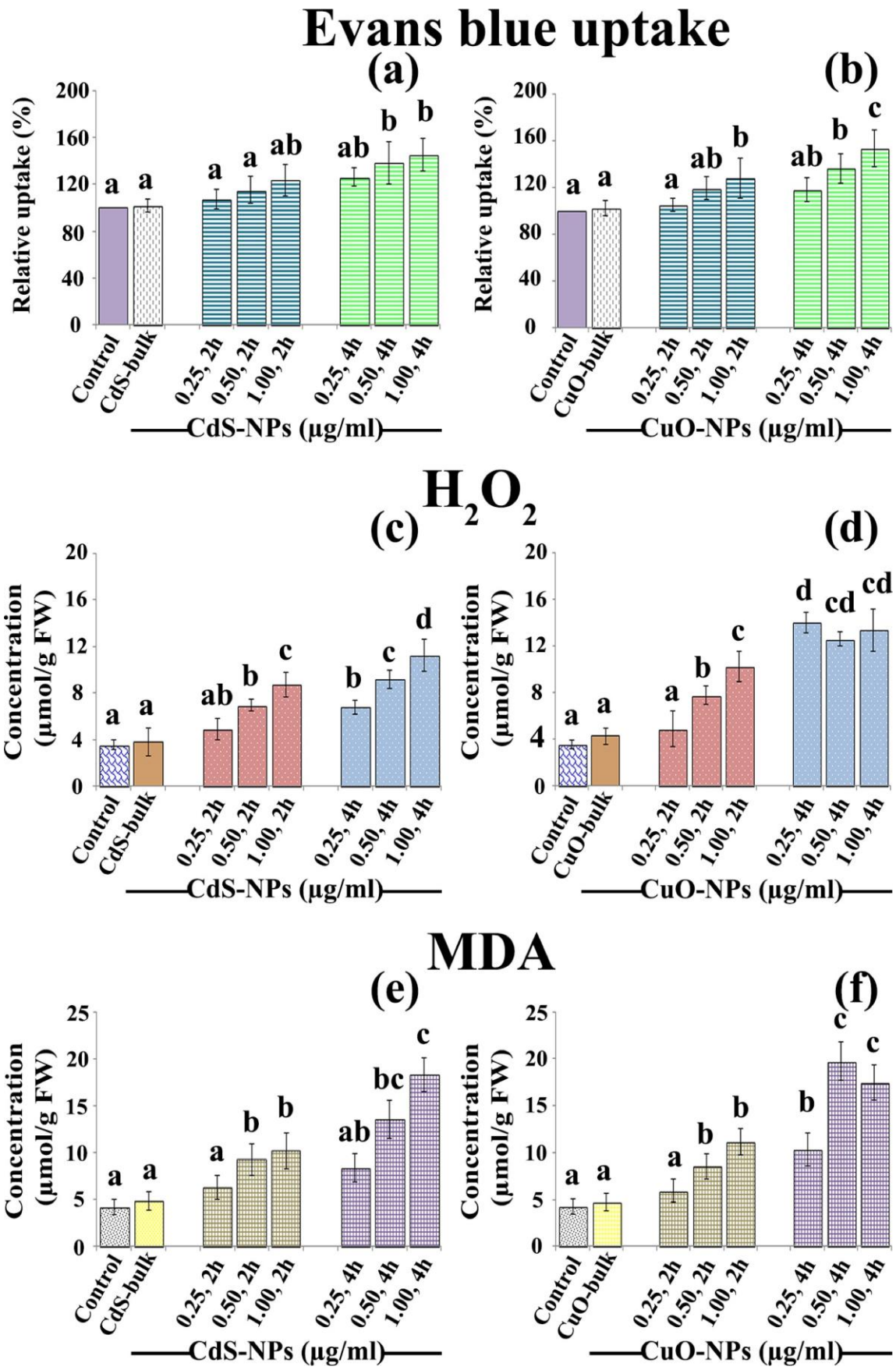

Figure 4: CdS- and CuO-NPs mediated stress in host. Evans blue uptake (a-b); H_2O_2 accumulation (c-d); MDA production (e-f)

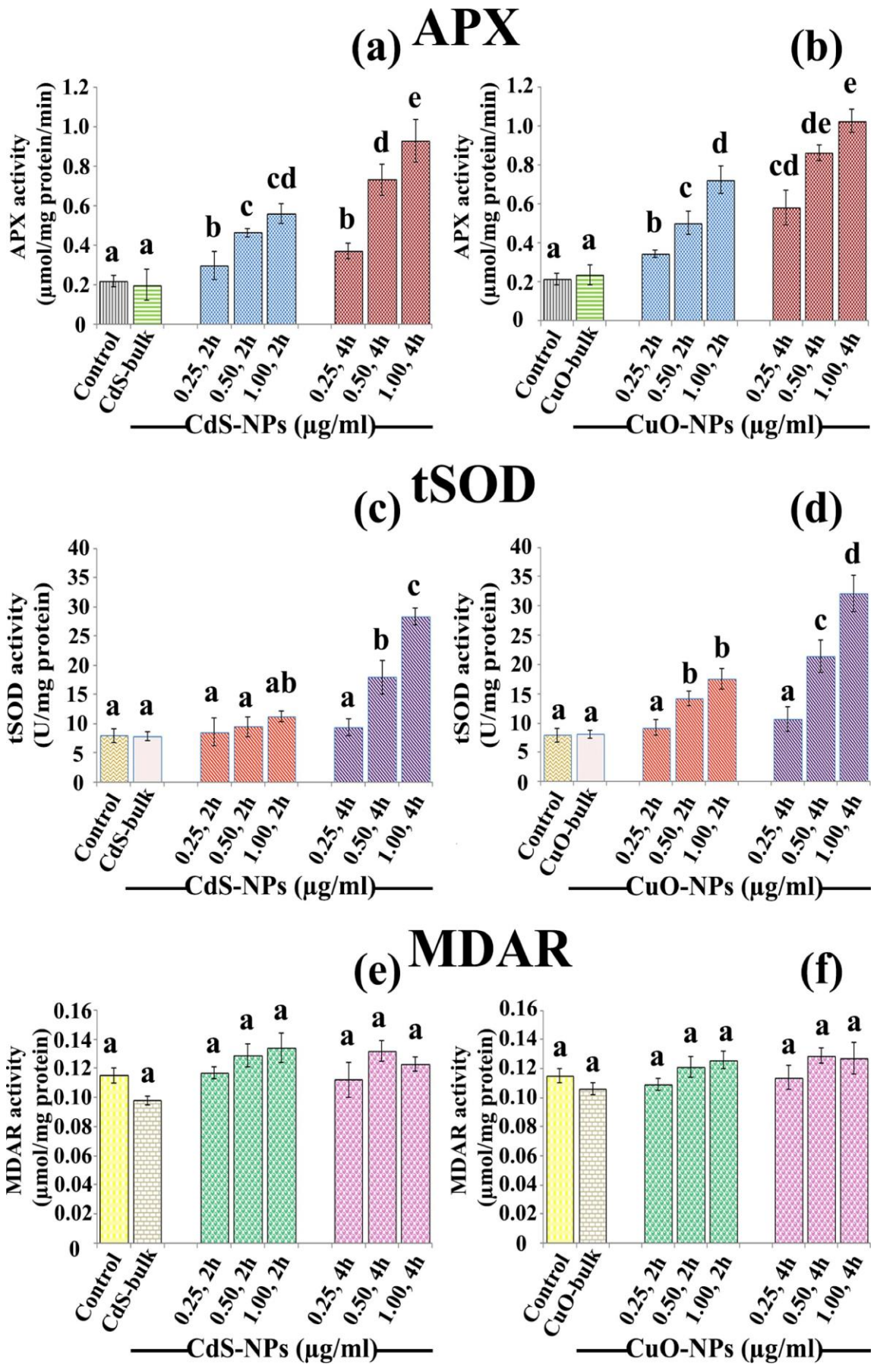

Figure 5: Antioxidant enzyme activity (APX: a-b; tSOD: c-d; MDAR: e-f) in host (*C. sativum*)

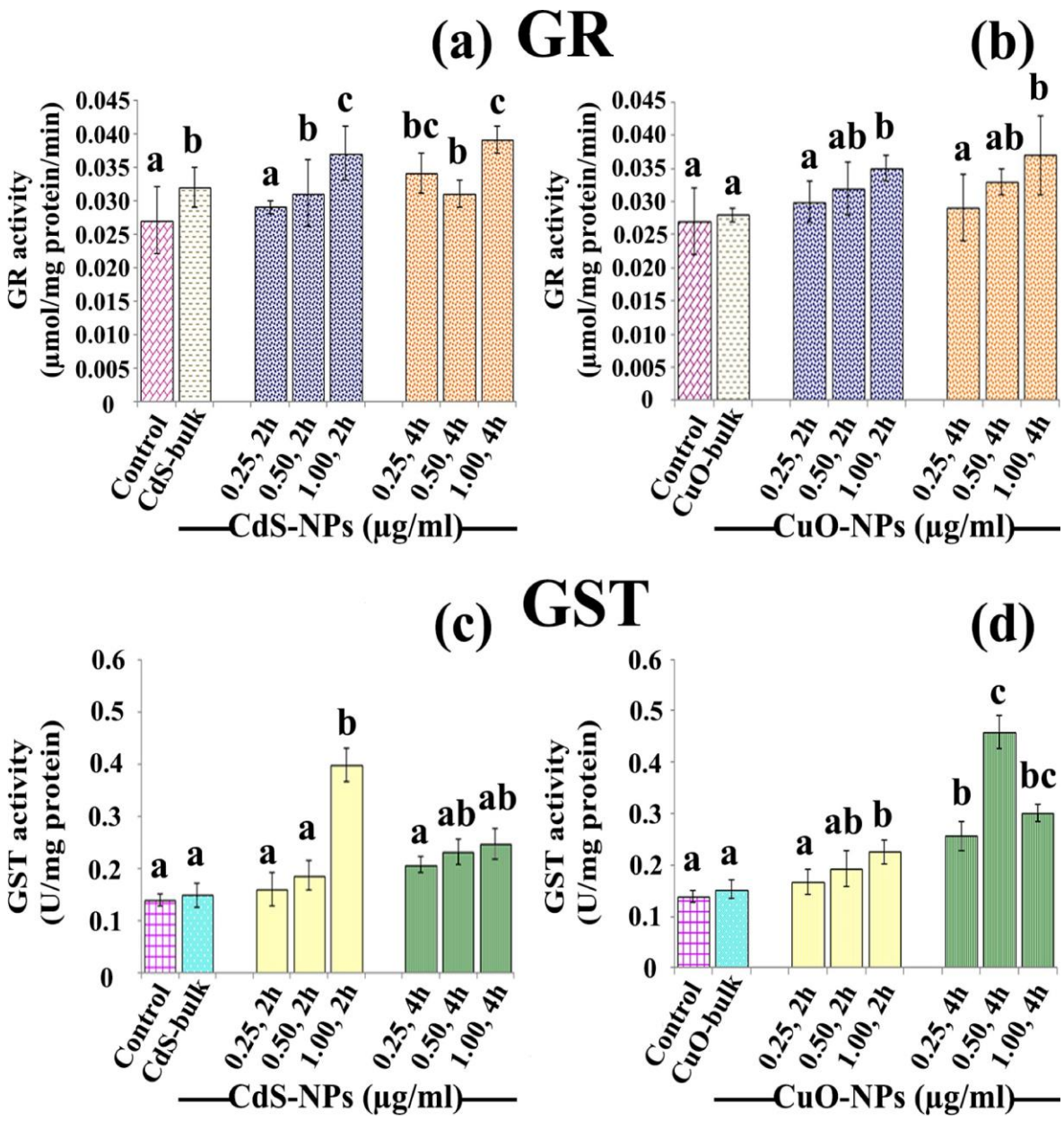

Figure 6: GR (a-b) and GST (c-d) activity in host cell

depression at 450-550 (Cd-S bonding), 1158-1422 (S-O bonding), 1526-1640 (S-H bonding) and 3400-3648 cm^{-1} (O-H stretching) wavelength regions for CdS-NPs (Fig. 1c) and 460-628 (Cu-O stretching), 1120-1280 (O-H bending vibration), 1580-1730 (C=O stretching bonds, C-H vibration) and 3240-3568 cm^{-1} (O-H stretching) spectrum regions for CuO-NPs (Fig. 1d) documenting differential bonding nature participating in nanocrystal formation. X-ray diffractogram of CdS-NPs records broad scattering peaks at 2θ values of 26.77º, 43.76º, 51.59º demonstrating existence of (1, 1, 1), (2, 2, 0) and (3, 1, 1) nanocrystal faces (Fig. 2a); while X-ray scattering plot of CuO-NPs exhibits sharp intense peaks at 35.66º, 38.61º, 49.09º (Fig. 2b) confirming persistence of reflection from (1, 1, 1) and (2, 0, 2) crystal planes. Study of particle brownian motion under DLS reveals mean hydrodynamics diameters of CdS- and CuO-NPs measured to be 36.0 ± 9.3 nm (range: 27.9 to 115.7 nm) and 98.0 ± 25.0 nm (71.9 to 340.5 nm) respectively (Fig. 2c-d). Low polydispersity index value (CdS-NPs: 0.497; CuO-NPs: 0.156) confirms monodispersion nature (Saha et al., 2011; Masarudin et al., 2015) of both the prepared nanosuspension. Surface scanning of CdS-NPs following field emission scanning electron microscope visually establishes spherical nature of solid nanocrystals (Fig. 2e); while study involving CuO-NPs exhibits elliptical to oval shaped nanoparticles (Fig. 2f). Size of both the NPs under FESEM (CdS-NPs: 20.0 to 80.0 nm; mean: 42.76 ± 14.28 nm; CuO-NPs: 10.0 to 90.0 nm (mean: 57.86 ± 18.79 nm) is nearly corroborating with DLS results. The size of bulk CdS and CuO is 13.6 ± 7.3 µm and 28.8 ± 9.8 µm respectively.

Study comprising opto-physical characterization of the engineered nanomaterials highlights quality of the prepared materials in the nanoscale dimension.

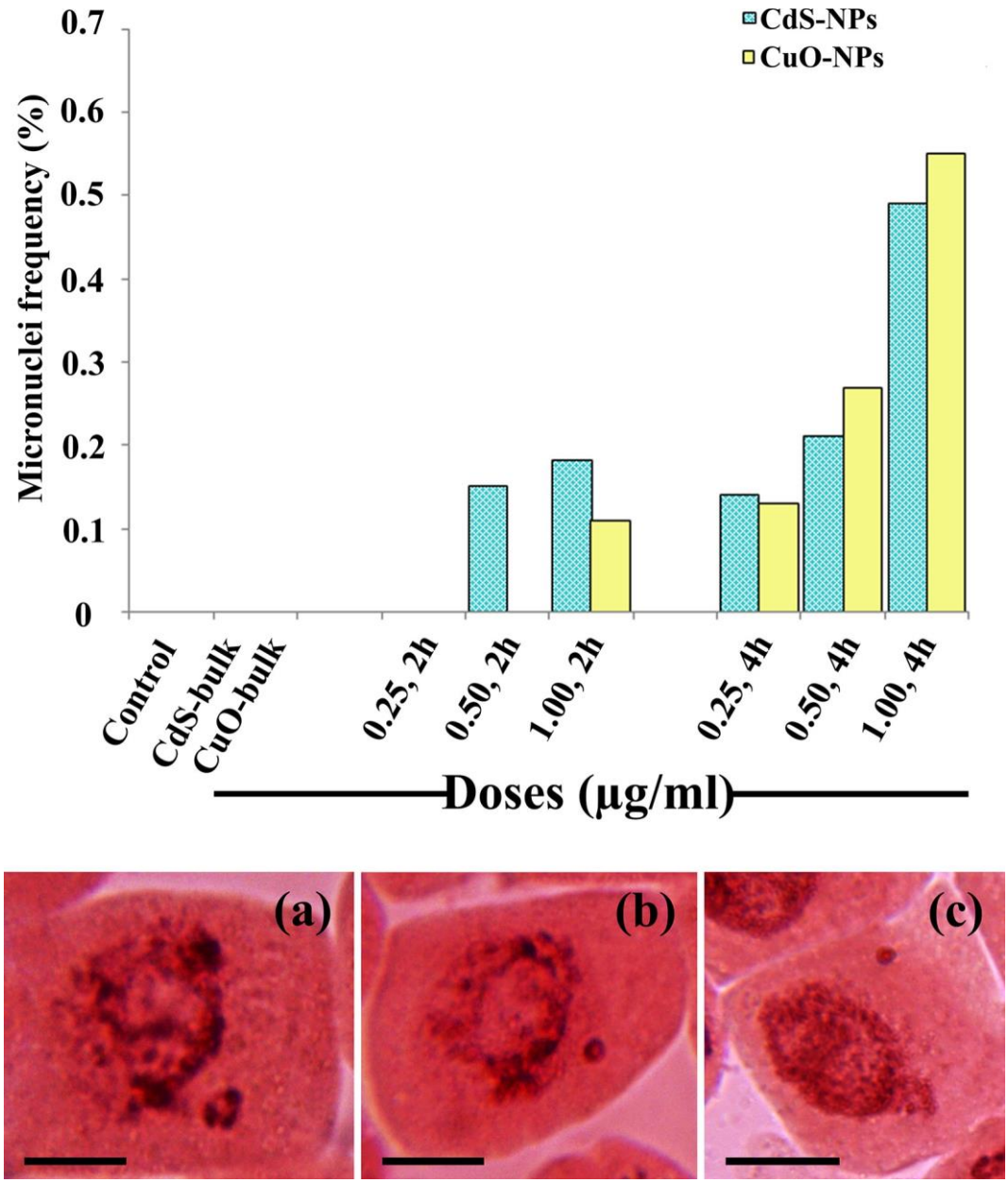

Figure 7: Bar histogram showing frequency of micronuclei in NPs treatments. Resting cells documenting un-condensed (a) and condensed (b-c) micronuclei of variable sizes. Scale bar = 10 µm

NPs accumulation in seedlings

CdS and CuO-NPs accumulation (µg/g) in seedlings (Fig. 3a-b) is dose dependent (detected in the form of metallic c ations). Taylor et al. (2014) opined that dose dependent uptake of NPs is due to passive entry of the nanomaterials in the biological system. Low amount of accumulations is also observed in bulk controls. NPs size, chemical nature, surface charge potentiality and monodisperse nature of nano-suspension are the contributing factors for passive uptake and accumulations of NPs in host system (Rico et al., 2011; Kettler et al., 2014). In the present investigation, uptake of nanomaterials is higher in 4 h treatment than 2 h. On comparative basis, lower doses (0.25 µg/ml and 0.50 µg/ml, 2 h) of CdS-NPs show enhance uptake than CuO-NPs which can be attributed to particle sizing effect. However in higher doses (1.00 µg/ml, 4 h), uptake of CdS-NPs is less than CuO-NPs and it can be possibly due to higher agglomeration potentiality of CdS-NPs. Therefore, nano-crystal stability in the capping suspension is an important contributing factor of NPs uptake. NPs uptake is essential for bio-reactivity.

Oxidative stress induction by NPs

Root cell viability

NPs mediated root cell mortality is studied following enhance uptake of Evans blue and is found dose dependent and significant (p<0.05) in both the NPs treatments compared to controls (Fig. 4a-b). Enhance uptake is indicative of cellular stress. Plant under stress condition stimulates cell wall lignification resulting in root growth inhibition (Passardi et al., 2005).

Oxidative stress

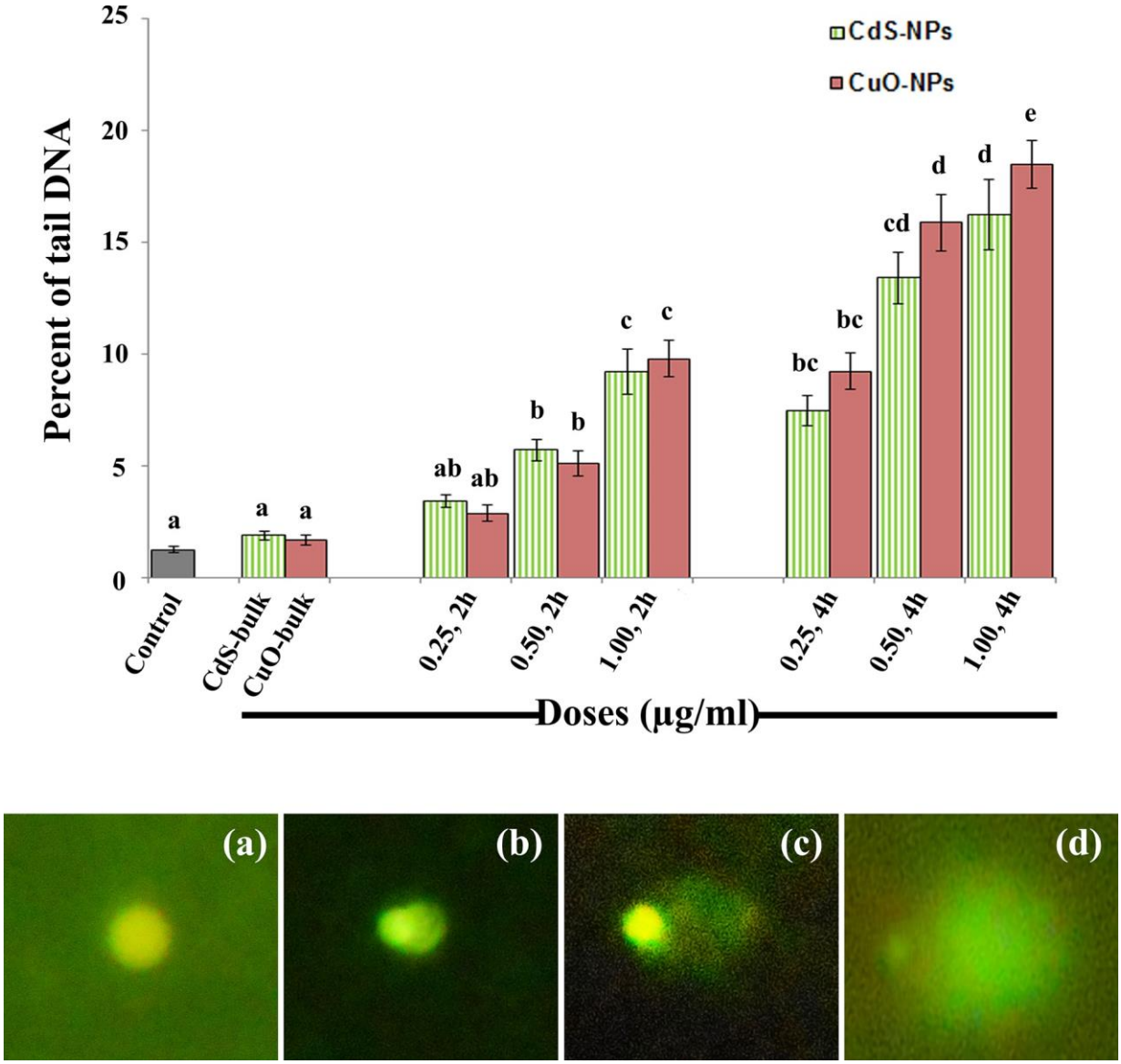

Figure 8: Bar histogram representing tail DNA percentage in controls and in NPs treatments. Normal nuclei (a) with comet photomicrographs (% tail DNA) in NPs treatments (b-d)

In relation to controls, accumulation of H_2O_2 in CdS- and CuO-N Ps treatments (Fig. 4c-d) is significant (p<0.05) and mostly dose dependent (excepting CuO-NPs: 0.50 µg/ml and 1.00 µg/ml, 4 h). Higher H_2O_2 generation in treatments suggests generation of reactive oxygen species (ROS) in the cellular system. More or less similar response is also noted for MDA accumulation in seedlings. Enhancement in subcellular MDA production compared to controls (Fig. 4e-f) highlights NPs mediated lipid peroxidation in tissue system resulting in loss of plasma membrane integrity (Oliveira and Schoffen., 2010) and subsequent induction of adverse effect on over all cellular health.

Antioxidant enzyme responses

In relation to controls, APX activity is dose dependent in both CdS- and CuO-NPs (Fig. 5a-b) and show significant (p<0.05) enhancement suggesting successful activation of initial step associated with ascorbate pool recycling (Massot et al., 2013). At comparable doses, CuO-NPs exhibit more pronounced APX kinetics than CdS-NPs. Results show near collinearity among the attributes like, nanoparticles uptake, H_2O_2 accumulation and APX activity for both the studied NPs. Compared to controls, elevation in tSOD activity (Fig. 5c-d) is found significantly (p<0.05) higher in 0.50 µg/ml and 1.00 µg/ml, 4 h CdS-NPs and 0.50 µg/ml and 1.00 µg/ml, 2 and 4 h CuO-NPs. CuO-NPs show relatively enhance tSOD activity than CdS-NPs at comparable doses. Increase in cellular tSOD concentration in NPs treatments (higher doses) demonstrates potential activation of secondary defense response mediated host protection network (Ishiga et al., 2009). MDAR activity is found insignificant between controls and NPs treatments (Fig. 5e-f) suggesting insufficient conversion of oxidized ascorbate to its reduced form and subsequent persistent of cellular stress

(Eastmond., 2007). Compared to controls, GR activity enhances only in the highest employed concentration (1.00 µg/ml) of both the durations of CdS- and CuO-NPs (Fig. 6a-b); while, elevation in GST kinetics (Fig. 6c-d) is found in 1.00 µg/ml, 2 h CdS-NPs and in all doses of 4 h treatments (including 1.00 µg/ml, 2 h of CdS-NPs).

Assessment of five antioxidant enzyme kinetics highlights disproportionate functioning of defense mechanism indicating prevalence of stress environment in the host. CuO-NPs is found to trigger relatively enhance defense response than CdS-NPs which is however, contrary with the size of synthesized NPs. This signifies that possibly smaller sized nanoparticles possess high tendency of agglomeration in the cellular environment.

Genotoxicity

Prevalence of oxidative stress in the cellular environment damages both chromosome and DNA (Khanna et al., 2015). Micronuclei formation in somatic cell highlights chromosomal damage; while, tail DNA percentage assessed from comet assay is attributed to DNA double strand breakage.

Detection of micronuclei

Micronuclei (Fig. 7a-c) both condensed and uncondensed types (mostly 1 and very rarely 2) of variable sizes (range: 1.71 µm to 3.26 µm) are found to occur in different doses of CdS-NPs (0.50 µg/ml, 2 h to 1.00 µg/ml, 4 h; range – 0.15% to 0.49%) and CuO-NPs (1.00 µg/ml, 2 h to 1.00 µg/ml, 4 h; range – 0.11% to 0.55%). No micronuclei could be detected in resulting cells of controls and initial doses of NPs treatments. Micronuclei are the outcome of chromosomal breakage in the dividing phase of cell division and their size and number are reflection of the extent of breakage (Evans et al., 1959; Kumbhakar et al., 2016).

Measurement of DNA double strand break

Double stranded DNA break is measured from tail DNA percentage following alkaline comet assay (Pourrut et al., 2015; Santos et al., 2015). Although controls (dry control – 1.25% ± 0.12; CdS-bulk – 1.87% ± 0.19; CuO-bulk – 1.68% ± 0.21) show tail DNA, percentage of tail DNA (Fig. 8a-d) is significant (p<0.05) mostly in treatments (0.50 µg/ml, 2 h to 1.00 µg/ml, 4 h). Tail DNA percentage among the treatments is found to vary from 3.41% ± 0.29 to 16.22% ± 1.56 in CdS-NPs and 2.87% ± 0.37 to 18.47% ± 1.07 in CuO-NPs.

CONCLUSION

Results suggest that oxidative stress though triggers defense reaction in host, NPs mediated cellular stress environment persists resulting in DNA damage (Xi et al., 2004). Such damage can bring about genome alteration (Vidal et al., 2001; Nel et al., 2006) and can be fixed into mutation (Singh et al., 2009; Langie et al., 2015). Furthermore, NPs mediated toxicity assessment can be potentially used to inhibit growth and cell division of human pathogenic microorganisms (Shrivastava et al., 2007; Kumbhakar et al., 2017) suggesting the role of nanomaterials in pharmacological applications.

ACKNOWLEDGMENTS

Authors are thankful to UGC consortium Center, Center for Research in Nanoscience and Nanotechnology (CRNN), University of Calcutta, Kalyani University for instrumentation facilities.

REFERENCES

Aebi, H. Catalase. 1983. In: Bergmeyer, H.U. Methods in Enzymatic Analysis (second English ed.), pp. 276 – 286. Academic Press, New York.

Ali, D., Alarifi, S., Alkahtani, S., AlKahtane, A.A., Almalik, A. 2015. Cerium oxide nanoparticles induce oxidative stress and genotoxicity in human skin melanoma cells. Cell Biochem. Biophys., 71(3), 1643 – 1651.

Beyer, W.F., Fridovich, I. 1987. Assaying for superoxide dismutase activity: some large consequences of minor changes in conditions. Anal. Biochem., 161(2), 559 – 566.

Brennan, T., Frenkel, C. 1977. Involvement of hydrogen peroxide in the regulation of senescence in pear. Plant Physiol., 59(3), 411 – 416.

Carlberg, I., Mannervik, B. 1985. Glutathione reductase assay. Methods in Enzymol. Academic Press, Orlando FL, 113, 484 – 495.

Dagher,S., Haik, Y., Ayesh, A.I., Tit, N. 2014. Synthesis and optical properties of colloidal CuO nanoparticles. J. Lumin., 151, 149 – 154.

Das, D., Datta, A.K., Kumbhakar, D.V., Ghosh, B., Pramanik, A., Gupta, S., Mandal, A. 2017. Assessment of photocatalytic potentiality and determination of ecotoxicity (using plant model for better environmental applicability) of synthesised copper, copper oxide and copper-doped zinc oxide nanoparticles. PLoS ONE, 12(8), e0182823.

Dobrzyńska, M.M., Gajowik, A., Radzikowska, J., Lankoff, A., Dušinská, M. and Kruszewski, M. 2014. Genotoxicity of silver and titanium dioxide nanoparticles in bone marrow cells of rats *in vivo*. Toxicol., 315(2014), 86 – 91.

Duchaniya, R.K. 2014. Optical studies of chemically synthesis CdS nanoparticles. International Journal of Mining, Metallurgy & Mechanical Engineering, 2(2), 54 – 56.

Eastmond, J. 2007. Monodehyroascorbate reductase4 is required for seed storage oil hydrolysis and post germinative growth in *Arabidopsis*. The Plant Cell, 19(4), 1376 – 1387.

Evans, H.J., Neary, G.J., Williamson, F.S. 1959. The relative biological efficiency of single doses of fast neutrons and gamma-rays on *Vicia faba* roots and the ef-

fect of oxygen. Part II. Chromosone damage: the production of micronuclei. Int. J. Radiat. Biol. Relat. Stud. Phys. Chem. Med., 1, 216 – 229.

Fahmy, B., Cormier, S.A. 2009. Copper oxide nanoparticles induce oxidative stress and cytotoxicity in airway epithelial cells. Toxicol. In Vitro, 23(7), 1365 – 71.

Ghosh, B., Datta, A.K., Pramanik, A., Kumbhakar, D.V., Das, D., Paul, R., Biswas, J. 2017. Mutagenic effectivity of cadmium sulphide and copper oxide nanoparticles on some physiological and cytological attributes of *Lathyrus sativus* L. Cytologia, 82(3), 1 – 5.

Ghosh, M., Bandyopadhyay, M., Mukherjee, A. 2010. Genotoxicity of titanium dioxide (TiO_2) nanoparticles at two trophic levels: plant and human lymphocytes. Chemosphere, 81(10), 1253 – 1262.

Halder, S., Mandal, A., Das, D., Datta, A.K., Chattopadhyay, A.P., Gupta, S., Kumbhakar, D.V. 2015. Effective potentiality of synthesised CdS nanoparticles in inducing genetic variation on *Macrotyloma uniflorum* (Lam.) Verdc. BioNanoSci., 5(3), 171 – 180.

Heath, R.L., Packer, L. 1968. Photoperoxidation in isolated chloroplasts. I. Kinetics and stoichiometry of fatty acid peroxidation. Arch. Biochem. Biophys., 125(1), 189 – 198.

Ishiga Y., Uppalapati S.R., Ishiga T., Elavarthi S., Martin B., Bender C.L. 2009. The phytotoxin coronatine induces light-dependent reactive oxygen species in tomato seedlings. New Phytol., 181(1), 147 – 160.

Kettler, K., Veltman, K., van de Meent, D., van Wezel, A., Hendriks, A.J. 2014. Cellular uptake of nanoparticles as determined by particle properties, experimental conditions, and cell type. Environ. Toxicol. Chem., 33(3), 481 – 492.

Khanna, P., Ong, C., Bay, B.H., Baeg, G.H. 2015. Nanotoxicity: An interplay of oxidative stress, inflammation and cell death. Nanomaterials, 5(3), 1163 – 1180.

Kumbhakar, D.V., Datta, A.K., Das, D., Sahu, V.P., Barbuddhe, S.B., Sharma, S., Ghosh, B.**,** Pramanik, A. 2017. Nano particle (metallic copper and cadmium sulphide) application: photocatalytic potentiality and antimicrobial effectivity. Indian J. Sci. Technol., 10(34), DOI: 10.17485/ijst/2017/v10i34/116671.

Kumbhakar, D.V., Datta, A.K., Mandal, A., Das, D., Gupta, S., Ghosh, B., Halder, S., Dey, S. 2016. Effectivity of copper and cadmium sulphide nanoparticles in mitotic and meiotic cells of *Nigella sativa* L. (black cumin) – can nanoparticles act as mutagenic agents? J. Exp. Nano. Sci., 11(11), 823 – 829.

Langie, A.S., Azqueta, A., Collins, A.R. 2015. The comet assay: past, present, and future. Front. Genet., 6, 1 – 3.

Lidén, G. 2011. The European commission tries to define nanomaterials. Ann. Occup. Hyg., 55(1), 1 – 5.

Manke, A., Wang, L., Rojanasakul, Y. 2013. Mechanisms of nanoparticle-induced oxidative stress and toxicity. BioMed. Res. Int., 2013, 1 – 15.

Masarudin, M.J., Cutts, S.M., Evison, B.J., Phillips, D.R., Pigram, P.J. 2015. Nanoparticles as candidate vectors for anticancer drug delivery: application to the passive encapsulation of [14C]-doxorubicin. Nanotechnol. Sci. Appl., 8, 67–80.

Massot, C., Bancel D., Lopez Lauri F., Truffault V., Baldet P., Gautier, H. 2013. High temperature inhibits ascorbate recycling and light stimulation of the ascorbate pool in tomato despite increased expression of biosynthesis genes. PLOS ONE, 8(12), e84474.

Miyake, C., Asada, K. 1992. Thylakoid-bound ascorbate peroxidase in spinach chloroplasts and photo reduction of its primary oxidation product monodehydroascorbate radicals in thylakoids. Plant Cell Physiol., 33(5), 541 – 553.

Nakano, Y., Asada, K. 1981. Hydrogen peroxide is scavenged by ascorbate specific peroxidase in spinach chloroplasts. Plant Cell Physiol., 22(5), 867 – 880.

Nel, A., Xia, T., Madler, L., Li, N. 2006. Toxic potential of materials at the nanolevel. Science, 311, 622 – 627.

Nowack, B., Bucheli, T.D. 2007. Occurrence, behavior and effects of nanoparticles in the environment. Environ. Pollut., 150(1), 5 – 22.

Oliveira, M C., Schoffen, J.P.F. 2010. Oxidative stress action in cellular aging. Braz. Arch Biol. Technol., 53(6), 1333 – 1342.

Passardi, F., Cosio, C., Penel, C., Dunand, C. 2005. Peroxidases have more functions than a Swiss army knife. Plant Cell Rep., 24(5), 255 – 265.

Pathak, N.L., Kasture, S.B., Bhatt, N.M., Rathod, J.D. 2011. Phytopharmacological properties of *Coriandrum sativum* as a potential medicinal tree: an overview. J. Appl. Pharm. Sci*,* 1(4), 20 – 25.

Pourrut, B., Pinelli, E., Celiz Mendiola, V., Silvestre, J., Douay, F. 2015. Recommendations for increasing alkaline comet assay reliability in plants. Mutagenesis, 30(1), 37 – 43.

Rajeshwari, U., Andallu, B. 2011. Medicinal benefits of coriander (*Coriandrum sativum* L). Spatula DD 1(1), 51 – 58.

Rico, C.M., Majumdar, S., Duarte-Gardea, M., Peralta-Videa, J.R., Gardea-Torresdey, J.L. 2011. Interaction of nanoparticles with edible plants and their possible implications in the food chain. J. Agric. Food Chem., 59(8), 3485 – 3498.

Saha, R., Verma, P.K., Mitra, R.K. and Pal, S.K. 2011. Structural and dynamical characterisation of unilamellar AOT vesicles in aqueous solutions and their efficacy as potential drug delivery vehicle. Colloids Surf. B, 88(1), 345 – 353.

Santos, C.L.V., Pourrut, B., Ferreira de Oliveira, J.M.P. 2015. The use of comet assay in plant toxicology: recent advances. Front. Genet., 6, 1 – 18.

Shrivastava, S., Bera, T., Roy, A., Singh, G., Ramachandrarao, P., Dash, D. 2007. Characterization of enhanced antibacterial effects of novel silver nanoparticles. Nanotechnology, 18, 225103 – 225112.

Singh, N., Manshian, B., Jenkins, G.J.S., Griffiths, S.M., Williams, P.M., Maffeis, T.G.G., Wright, C.J., Doak, S.H. 2009. Nanogenotoxicology: The DNA damaging potential of engineered nanomaterials. Biomaterials, 30(23-24), 3891 – 3914.

Tamás, L., Šimonovičová, M., Huttová, J., Mistrík, I. 2004. Aluminium stimulated hydrogen peroxide production of germinating barley seeds. Environ. Exp. Bot., 51(3), 281 – 288.

Taylor, A.F., Rylott, E.L., Anderson, C.W., Bruce, N.C. 2014. Investigating the toxicity, uptake, nanoparticle formation and genetic response of plants to gold. PLoS One, 9(4), e93793.

Tervonen, T., Linkov, I., Figueira, J.R., Steevens, J., Chappell, M., Merad, M. 2009. Risk-based classification system of nanomaterials. J. Nanopart. Res., 11, 757 – 766.

Valencia-Quintana, R., Gómez-Arroyo, S., Sánchez-Alarcón, J., Milić, M., Olivares, J.L., Waliszewski, S.M., Cortés-Eslava, J., Villalobos-Pietrini, R., Calderón-Segura, M.E. 2016. Assessment of genotoxicity of Lannate-90® and its plant and animal metabolites in human lymphocyte cultures. Arh. Hig. Rada. Toksikol., 67(2), 116 – 125.

Ventura, L., Giovannini, A., Savio, M., Donà, M., Macovei, A., Buttafava, A., Carbonera, D., Balestrazzi, A. 2013. Single cell gel electrophoresis (comet) assay with plants: research on DNA repair and ecogenotoxicity testing. Chemosphere, 92(1), 1 – 9.

Vidal, A.E., Hickson, I.D., Boiteux, S., Radicella, J.P. 2001. Mechanism of stimulation of the DNA glycosylase activity of hOGG1 by the major human AP endonuclease: bypass of the AP lyase activity step. Nucl. Acids Res., 29(6), 1285 – 1292.s

Xi, Z.G., Chao, F.H., Yang, D.F., Sun, Y.M., Li, G.X., Zhang, H.S., Zhang, W., Yang, Y.H., Liu, H.L. 2004. The effects of DNA damage induced by acetaldehyde. Huan Jing Ke Xue, 25(3), 102 – 105.